Open Access Library Journal

Crystal Structural and Raman Vibrational Studies of $Bi_{1-x}Sb_{1-x}Te_{2x}O_4$ Solid Solution with $0 \leq x \leq 0.1$

Leila Loubbidi[1*], Abdeslam Chagraoui[1], Imane Yakine[1], Brahim Orayech[2], Mohamed Naji[3,4], Josu M. Igartua[2], Abdelmjid Tairi[1]

[1]Laboratoire de Physico, Chimie des Matériaux Appliqués, Département de Chimie, Faculté des Sciences Ben M'Sik, Université HassanII, Mohammedia Casablanca, Morocco
[2]Departamento de Física de la Materia Condensada, Universidad del País Vasco, Bilbao, Spain
[3]CNRS, UPR3079 CEMHTI, Orléans, France
[4]Faculté des Sciences, Université d'Orléans, Orléans, France
Email: [*]leila.loubbidi@gmail.com

Received 26 October 2014; revised 30 November 2014; accepted 21 December 2014

Abstract

Synthesis and crystal structures are described for the $Bi_{1-x}Sb_{1-x}Te_{2x}O_4$ solid solution with $0 \leq x \leq 0.1$. It crystallizes in the monoclinic system, space group I2/c. Rietveld refinements of X-ray powder diffraction data indicate that the atomic positions are: $Bi/Te^{(2)}$(4c), $Sb/Te^{(1)}$(4d). The oxygen occupied two sites, 8f and 8b, respectively. The reliability factors are: R_p = 7.45%, R_{wp} = 10.6% and R_b = 3.88% for x = 0.1. The structure contains $[(Sb/Te^{(1)})O_4]_n$ layers formed by $(Sb/Te^{(1)})O_6$ octahedra sharing corners, which are parallel to (001) plan and held together by bismuth and tellurium atoms. The Raman study of this solid solution shows the bands which are assigned to O-Bi^{3+}-O, O-Sb^{5+}-O and connects $(Bi/Te^{(2)})O_8$-$(Sb/Te^{(1)})O_6$ vibration in the crystal.

Keywords

$BiSbO_4$, TeO_2, Crystal Structure, Spectroscopy Raman

Subject Areas: **Analytical Chemistry, Composite Material**

1. Introduction

After the intense research activity during last years, the XRD analysis of the $A^{3+}B^{5+}O_4$ compositions (A = Bi^{3+} or

[*]Corresponding author.

How to cite this paper: Loubbidi, L., Chagraoui, A., Yakine, I., Orayech, B., Naji, M., Igartua, J.M. and Tairi, A. (2014) Crystal Structural and Raman Vibrational Studies of $Bi_{1-x}Sb_{1-x}Te_{2x}O_4$ Solid Solution with $0 \leq x \leq 0.1$. *Open Access Library Journal*, **1**: e1180. http://dx.doi.org/10.4236/oalib.1101180

Sb^{3+}, and B = Nb^{5+}, Sb^{5+} or Bi^{5+}) showed that the compounds were isostructural, though various modifications were possible [1]-[3]. It is worthy to highlight the valence instability of Sb^{3+} cations during sintering course in air atmosphere (Sb^{3+} is easy to be oxygenized to Sb^{5+}). In recent studies, the authors reported the good microwave dielectric properties of $BiSbO_4$ and $Bi(Sb,Ta)O_4$ ceramics [4] [5]. $BiSbO_4$ was also reported in detail as a novel p-block metal oxide, which possessed a visible light response for photocatalytic degradation of methylene blue by Xin P. Lin *et al*. [6].

Kinnedy [7] reported a Rietveld refinement of X-ray powder diffraction study of $BiSbO_4$ and found that it belonged to a monoclinic structure with the space group I2/c.

As reported by Tairi *et al*. [8], the solid solution phase $Bi^{III}_{1-x}Sb_x^{III}Sb^{V}O_4$ exists in the composition range $0 \leq x \leq 1$. Depending on the composition taken in the field Bi_2O_3-$BiSbO_4$, authors have delineated several phases: α-Bi_2O_3, Bi_3SbO_7 and $BiSbO_4$.

The study of this pseudo-binary was later extended by M. Miyayama and H. Yanagida [9] to the whole system. He also confirmed that the existence of particular phases obtained Bi_3SbO_7, $BiSbO_4$ and a continuous solid solution between $BiSbO_4$-Sb_2O_4. High-temperature mass spectrometric vaporization study of the Bi-Sb-O system has been investigated by N. A. Gribchenkova *et al*. [10]. However, the characteristics and the compositions in the system Bi-Sb-O doped with TeO_2 have not been investigated sufficiently in the literature. Based on the studies on $A^{3+}B^{5+}O_4$ compositions (A = Bi^{3+} or Sb^{3+}, and B = Nb^{5+}, Sb^{5+} or Bi^{5+}) family's properties and structures, it attracts us to study the phase relationship between $BiSbO_4$ and TeO_2 solid solution. The investigation devoted to the compounds having cations with stereochemical active pair electrons as bismuth, tellurium and antimony, precise information on bond lengths and sites occupations will contribute to the understanding of its structural chemistry. It is therefore the aim of this paper to report the development on the structural properties in pseudo-binary $BiSbO_4$-TeO_2.

2. Experimental

The standard method of solid-state chemical reaction was applied to synthesize the $Bi_{1-x}Sb_{1-x}Te_{2x}O_4$ compounds. Proper stoichiometric molar ratios of the starting compounds were mixed using the starting compounds Bi_2O_3 (99.99%), TeO_2 (99.999%) and Sb_2O_3 (99.995%). The starting materials were mixed and ground in an agate mortar and heated in air in alumina crucibles. The following heat treatment procedure was used: 24 h at 600˚C, 24 h at 700˚C and 48 h at 850˚C. After each heating treatment, the sample was cooled down to room temperature, slowly at 3˚C/min and re-ground (re-mixed) to improve homogeneity. X-ray diffraction measurements were performed after each heat treatment to check the quality of the obtained materials.

Room temperature X-ray powder diraction data were obtained Bruker D8 high resolution diffractometer, the CuKα1 (λ = 1.5406 Å) wave length was used. The full pattern refinements were carried out by the Rietveld method with the FullProf program integrated in Winplotr software. The Rietveld refinement of the observed powder XRD data is initiated with scale and background parameters, and, successively, other profile parameters are included. The background is fitted with a fifth order polynomial. The peak shape is fitted with a Pseudo-Voigt profile function. After an appreciable profile matching, the position parameters and isotropic atomic displacement parameters of individual atoms were also refine.

Experiments have been carried out using Raman spectra were recorded in the 80 - 1000 cm^{-1} range using a Horiba Jobin-è-spectrometer (T64000 model) equipped with an Ar^+ laser (514.5 nm exciting line) and a CCD detector in a backscattering geometry. The incident laser beam was focused with the spot size of less than 5 μm by the objective (×100) to excite the sample. The spectra were recorded in two scans (during 100 s) at low power (<100 mW) of the excitation line, in order to avoid local heating of the sample. The spectral resolution was about 2.5 cm^{-1} at the exciting line.

3. Results and Discussion

3.1. Room-Temperature Crystal Structure Analysis

In our recent investigation in Bi_2O_3-TeO_2-Sb_2O_3 (Sb_2O_5) system, the existence of a solid solution with formulation $Bi_{1-x}Sb_{1-x}Te_{2x}O_4$ ($0 \leq x \leq 0.1$) have been synthesized [11]. Based on the analysis XRD of $Bi_{1-x}Sb_{1-x}Te_{2x}O_4$ we can distinguish two regions. In the ($0 \leq x \leq 0.1$) region all the compositions belongs to monoclinic structure isotype to $BiSbO_4$. The compositions with x = 0, 0.05 and 0.1 labeled A, B and C respectively are represented in

Figure 1. Typical X-ray diffraction patterns of them are shown in **Figure 2** and the lattice parameters derived from the XRD patterns are listed in **Table 1**. This solid solution is obtained at 850˚C (48 h). **Table 1** shows the cell parameters and the volume evolution of the monoclinic cell with the composition. The substitution of antimony atoms and bismuth by tellurium in the network $BiSbO_4$ has no significant influence on the lattice parameters evolution. The average size of the substituted atoms (Sb and Bi) atoms by tellurium is essentially the same: $[(0.1 \times rBi^{3+}) + (0.1 \times rSb^{5+}) \cong (2 \times 0.1 \times rTe^{4+})]$; rSbV = 0.60 Å [6], rTe^{4+} = 0.97 Å [6] and rBiIII = 1.31 Å [8]. In second region (x > 0.1), the XRD patterns shows mixed phases, limit of solid solution and phase belongs in the pseudo binary (Bi_2O_3-TeO_2) or Bi_2O_3-Sb_2O_3 (Sb_2O_5).

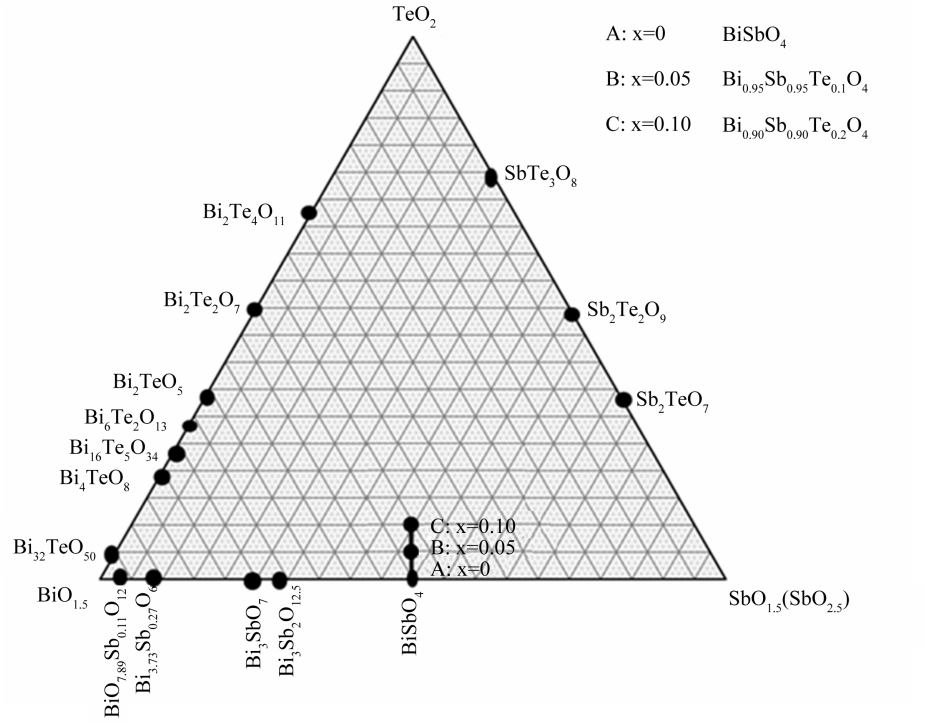

Figure 1. Ternary-Bi_2O_3-$TeO_2Sb_2O_3$ (Sb_2O_5) representing the different phases (straight black line represents the solid solution of $Bi_{1-x}Sb_{1-x}Te_{2x}O_4$with $0 \le x \le 0.1$).

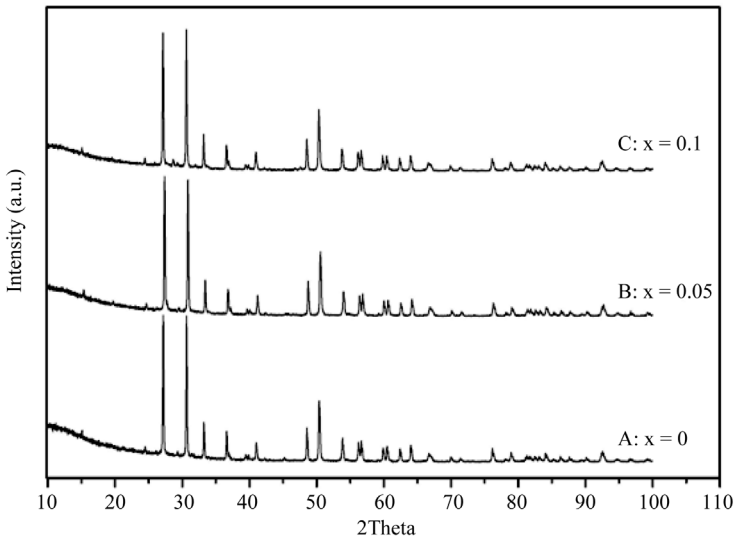

Figure 2. X-ray powder diffraction patterns of the compositions A, B and C.

Table 1. Cell parameters evolution of the solid solution $Bi_{1-x}Sb_{1-x}Te_{2x}O_4$ ($0 \le x \le 0.1$).

$Bi_{1-x}Sb_{1-x}Te_{2x}O_4$	a(Å)	b(Å)	c(Å)	β(°)	V(Å^3)
x = 0: (A) $BiSbTeO_4$	5.4690(5)	4.8847(2)	11.8252(6)	101.13(1)	310.00(2)
x = 0.05: (B) $Bi_{0.95}Sb_{0.95}Te_{0.1}O_4$	5.4694(5)	4.8868(2)	11.8218(6)	101.12(3)	310.05(2)
x = 0.10: (C) $Bi_{0.90}Sb_{0.90}Te_{0.2}O_4$	5.4625(5)	4.8808(2)	11.8143(6)	101.116(3)	309.08(2)

In order to have a details information on these materials, structure determination of the solid solution $Bi_{1-x}Sb_{1-x}Te_{2x}O_4$ (x = 0.1) was carried out by using Rietveld method. **Table 2** includes the crystallographic parameters, registration requirements and refinement parameters for $Bi_{0.90}Sb_{0.90}Te_{0.2}O_4$.

The first attempts of the structural refinement of the compound $Bi_{0.90}Sb_{0.90}Te_{0.2}O_4$ were made on the basis of a content distribution of the atomic lattice, *i.e.* the reduced coordinates of the initial atoms are those of $BiSbO_4$ phase [12]. Several hypotheses have been raised about the cations distribution. All divergent except where $Bi/Te^{(2)}$ and $Sb/Te^{(1)}$ atoms occupy the sites 4c and 4d respectively. Attempts to refine the atomics displacements ("thermal") parameters independently for both crystallographically non-equivalent O atoms were unsuccessful ([B_{iso}($O^{(I)}$ and $O^{(II)}$)] have the negative value of −0.52) and these parameters were constrained to be equal. We also tried to refine the SOF values for the $O^{(I)}$ and $O^{(II)}$ atoms mentioned in the previous section, along with the overall Biso value (because of extremely high correlations between the individual Biso and site occupation facteur (SOF) values, simultaneous refinement of these values for an atom in a structure is usually unsuccessful); but general improvement of the fit was not observed, and the site occupation facteur (SOF) values obtained 1.29(10) and (1) respectively, are consistent with the ideal value site occupation facteur 1. Taking these facts into account, the site occupation facteur values for $Sb/Te^{(1)}$, $Bi/Te^{(2)}$ and O in the structure were considered theoretical to be equal to 1.

After refinement, the reliability factors stabilize values: R_b = 3.88%, R_f = 3.66%, R_p = 7.23%, R_{wp} = 10.8%. The atomic coordinates and thermal factors refined agitation are given in **Table 3**. Observed, calculate and difference powder XRD patterns are given in **Figure 3**. The main interatomic distances and bond angles are summarized in **Table 4**.

Coming to the general architecture of $BiSbO_4$ that is drawn by using ATOMS program [13], which is isostructural with β-Sb_2O_4, it is possible to depict that is formed by $[SbO_4]_n$ layers built up by octahedra sharing corners hed together via bismuth atoms lying in (001) [7]. In **Figure 4** we have shown a perspective view of the contents of the atomic lattice and the various cations coordination. The structure of $Bi_{0.90}Sb_{0.90}Te_{0.2}O_4$ is formed by a three-dimensional network of octahedral $(Sb/Te^{(1)})O_6$ linked by the polyhedra $(Bi/Te^{(2)})O_8$.

Each $Sb/Te^{(1)}$ atom is surrounded by six oxygen atoms, two of them are normal distances being 2.000(2) Å, two short distances 1.949(2) Å and two others long distances at 2.076(2) Å. The corresponding polyhedron is a slightly distorted octahedron. The mean value $Sb/Te^{(1)}$-O is 2.008 Å which is in perfect accordance with the sum of radii as proposed by Shannon [14] and observed in others compounds such as β-Sb_2O_4 where Sb-O distances ranging from 1.97 to 2.0 Å [15] and $Sb_2Te_2O_7$ exhibiting $[Sb_2O_9]_n$ ribbons built up by regular SbO_6 octahedra, Sb-O distances show a wider range of values, from 1.91 to 2.03 Å [16] (**Table 4** and **Figure 5**). The octahedral are connected by the corners via the oxygen atom.

Each $(Bi/Te^{(2)})O_8$ square antiprism is connected with another square antiprism sharing $O_5^{(II)}$ and $O_6^{(II)}$ atoms to form a Bi_2O_{14} units as shown in **Figure 6**. The $Bi/Te^{(2)}$ atoms are surrounded by 8 oxygen atoms located at distances ranging from 2.147(2) Å to 2.865(2) Å (**Table 4**). We can distinguish three types of distances $Bi/Te^{(2)}$-O. Two distances anomaly long (2.865(2) Å) with the oxygen atoms $O_1^{(I)}$ and $O_2^{(I)}$. Two longer distances (2.756(2) Å) with $O_3^{(I)}$ and $O_4^{(I)}$. Four relatively short distances (2.147(2) Å and 2.322(2) Å) with the oxygen atoms $O_5^{(II)}$, $O_6^{(II)}$, $O_7^{(II)}$ and $O_8^{(II)}$. The average distance <$Bi/Te^{(2)}$-O> = 2.52 Å is in agreement with the sum of ionic radii proposed by Shannon [14]. The small disparity reveals a weak streochemical activity of the lone pair E of the $Bi/Te^{(2)}$ atom, classically directed opposite to the shorter Bi-O bonds; *i.e.* in the tetrahedron direction $O_5^{(II)}$-$O_6^{(I)}$-$O_7^{(II)}$-$O_8^{(II)}$. This result is comparable with previous phases such as Bi_2TeWO_{10}, $Bi_2Te_2W_3O_{16}$ and $Bi_2Te_5WO_{16}$ [17]-[19]. The $Bi/Te^{(2)}$ polyhedrons are shared by $O_5^{(II)}$-$O_6^{(II)}$ edges to constitute the chains parallel to Oy-axis (**Figure 4**). Their association in the three-dimensional framework let's consider hexagon cages which are located the $Sb/Te^{(1)}$ atoms (**Figure 6**).

Table 2. Structural data and Rietveld refinement parameters for $Bi_{0.90}Sb_{0.90}Te_{0.2}O_4$.

Formula	$Bi_{0.90}Sb_{0.90}Te_{0.2}O_4$
Crystal system	Monoclinic
Space group	I2/c
a(Å)	5.4625(5)
b(Å)	4.8808 (2)
c(Å)	11.8143(6)
θ(°)	101.116(3)
Volume (Å^3)	309.08(2)
Z	4
Radiation (Å)	Cu 1.5406$^{(\circ)}$
2θ scan range; step	17 - 80; 0.02
Scan speed	100 s/step
Number of independent parameters	77
Profile parameters R_F, R_P, R_{WP}	3.66%, 7.23%, 10.8%
Bragg R-factors (R_B)	3.88
Goodness of fit χ^2	1.51
R_{exp}	9.18

Table 3. Crystal structure data determined from Rietveld refinement for $Bi_{0.90}Sb_{0.90}Te_{0.2}O_4$.

Atome	Site	x	y	z	B_{iso}(Å^2)
Bi	4c	0	0.51177(10)	0.25	0.529(12)
$Te^{(2)}$	4c	0	0.51177(10)	0.25	0.539(12)
Sb	4d	0	0	0	0.519(17)
$Te^{(1)}$	4d	0	0	0	0.519(17)
$O^{(I)}$	8e	0.234(6)	0.295(6)	0.072(3)	0.278(5)
$O^{(II)}$	8e	0.106(6)	0.853(6)	0.155(3)	0.165(5)

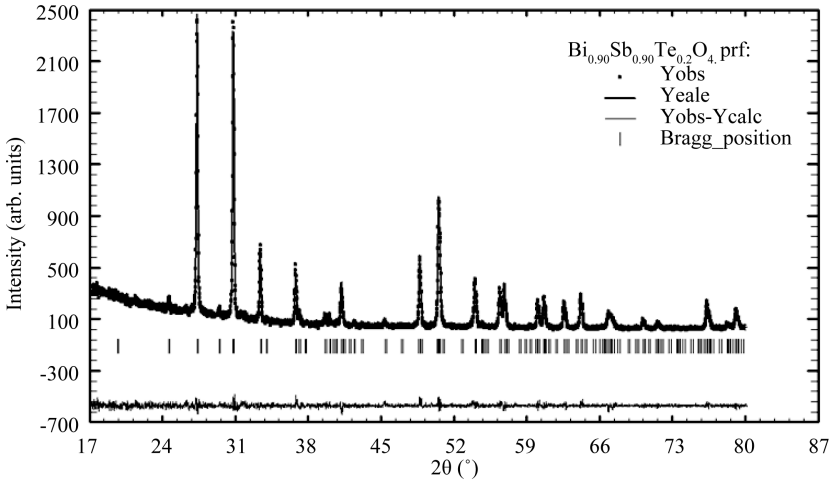

Figure 3. Final Rietveld plots for $Bi_{0.90}Sb_{0.90}Te_{0.2}O_4$. The upper symbols illustrate the observed data (circles) and the calculated pattern (solid line). The vertical markers show calculated positions of Bragg reflections. The lower curve is the difference diagram.

The atoms of Sb/$Te^{(1)}$ octahedral at the center of the cube and the center of the faces. The distribution of anions around each cation is highly anisotropic and characteristic of a strong streochemical activity of the electron lone pair E. It corresponds, if only the shortest distances are taken into account. The coupled substitution of Bi^{3+} ions

Table 4. Main interatomic distances (Å) angles (˚) and bond valence for $Bi_{0.90}Sb_{0.90}Te_{0.2}O_4$.

Sb/Te$^{(1)}$	$O_1^{(I)}$	$O_2^{(I)}$	$O_3^{(I)}$	$O_4^{(I)}$	$O_5^{(II)}$	$O_6^{(II)}$	Vij
$O_1^{(I)}$	**2.000(2)**	2.998(3)	4.005(3)	2.766(3)	2.525(3)	3.041(3)	0.85
$O_2^{(I)}$	94.62(15)	**2.076(2)**	2.766(3)	4.153(3)	2.992(3)	2.697(3)	0.69
$O_3^{(I)}$	180.00(17)	85.37(15)	**2.000(2)**	2.998(3)	3.041(3)	2.524(3)	0.85
$O_4^{(I)}$	85.37(15)	180.00(14)	94.62(15)	**2.076(2)**	2.697(3)	2.992(3)	0.69
$O_5^{(II)}$	79.39(14)	95.95(15)	100.70(16)	84.04(15)	**1.949(2)**	3.899(3)	0.98
$O_6^{(II)}$	100.60(16)	84.04(15)	79.39(14)	95.95(15)	180.00(14)	**1.949(2)**	0.98
∑Vij							**5.04**

⟨Sb/Te$^{(1)}$-O⟩ = 2.008 Å.

Bi/Te$^{(2)}$	$O_1^{(I)}$	$O_2^{(I)}$	$O_3^{(I)}$	$O_4^{(I)}$	$O_5^{(II)}$	$O_6^{(II)}$	$O_7^{(II)}$	$O_8^{(II)}$	Vij
$O_1^{(I)}$	**2.865(2)**	5.326(3)	4.199(3)	2.766(3)	3.023(3)	4.853(3)	3.607(3)	4.12(3)	0.12
$O_2^{(I)}$	136.67(14)	**2.865(2)**	2.766(3)	4.199(3)	4.853(3)	3.023(3)	4.121(3)	3.607(3)	0.12
$O_3^{(I)}$	96.62(12)	58.91(9)	**2.756(2)**	4.629(3)	4.480(3)	3.785(3)	2.526(3)	4.854(3)	0.16
$O_4^{(I)}$	58.91(9)	96.62(12)	114.19(10)	**2.756(2)**	3.785(3)	4.480(3)	4.853(3)	2.524(3)	0.16
$O_5^{(II)}$	72.57(17)	150.68(17)	131.58(15)	100.30(13)	**2.147(2)**	2.711(3)	2.676(3)	2.910(3)	0.84
$O_6^{(II)}$	150.68(12)	72.57(11)	100.30(13)	131.58(15)	78.28(15)	**2.147(2)**	2.910(3)	2.673(3)	0.84
$O_7^{(II)}$	87.46(15)	104.71(15)	58.874(10)	145.63(15)	73.34(13)	81.14(15)	**2.322(2)**	4.454(3)	0.57
$O_8^{(II)}$	104.71(15)	87.46(12)	145.636(15)	58.87(10)	81.14(10)	73.34(13)	147.01(14)	**2.322(2)**	0.57
∑Vij									**3.38**

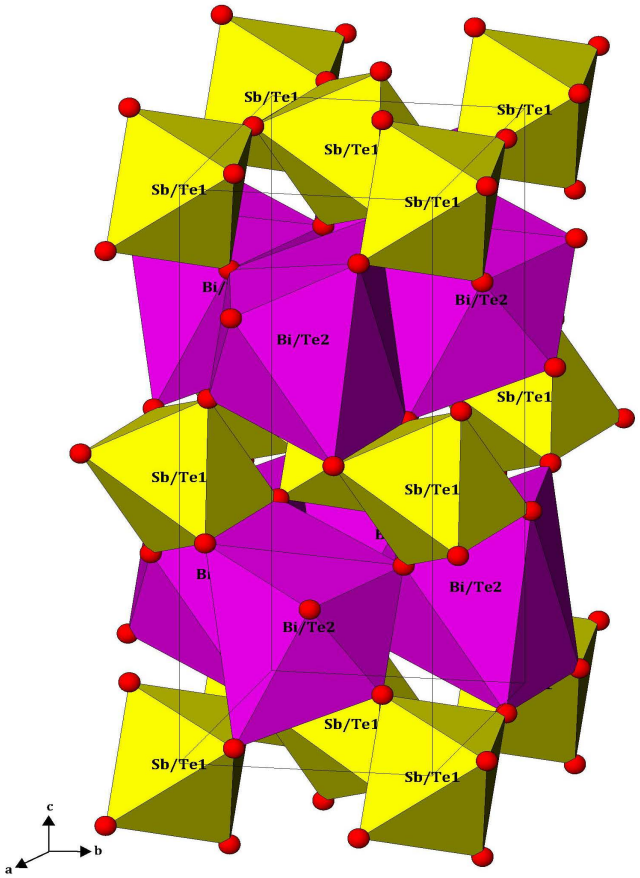

Figure 4. Three-dimensional view of $Bi_{0.90}Sb_{0.90}Te_{0.2}O_4$ unit cell illustrating the typical polyhedral arrangement.

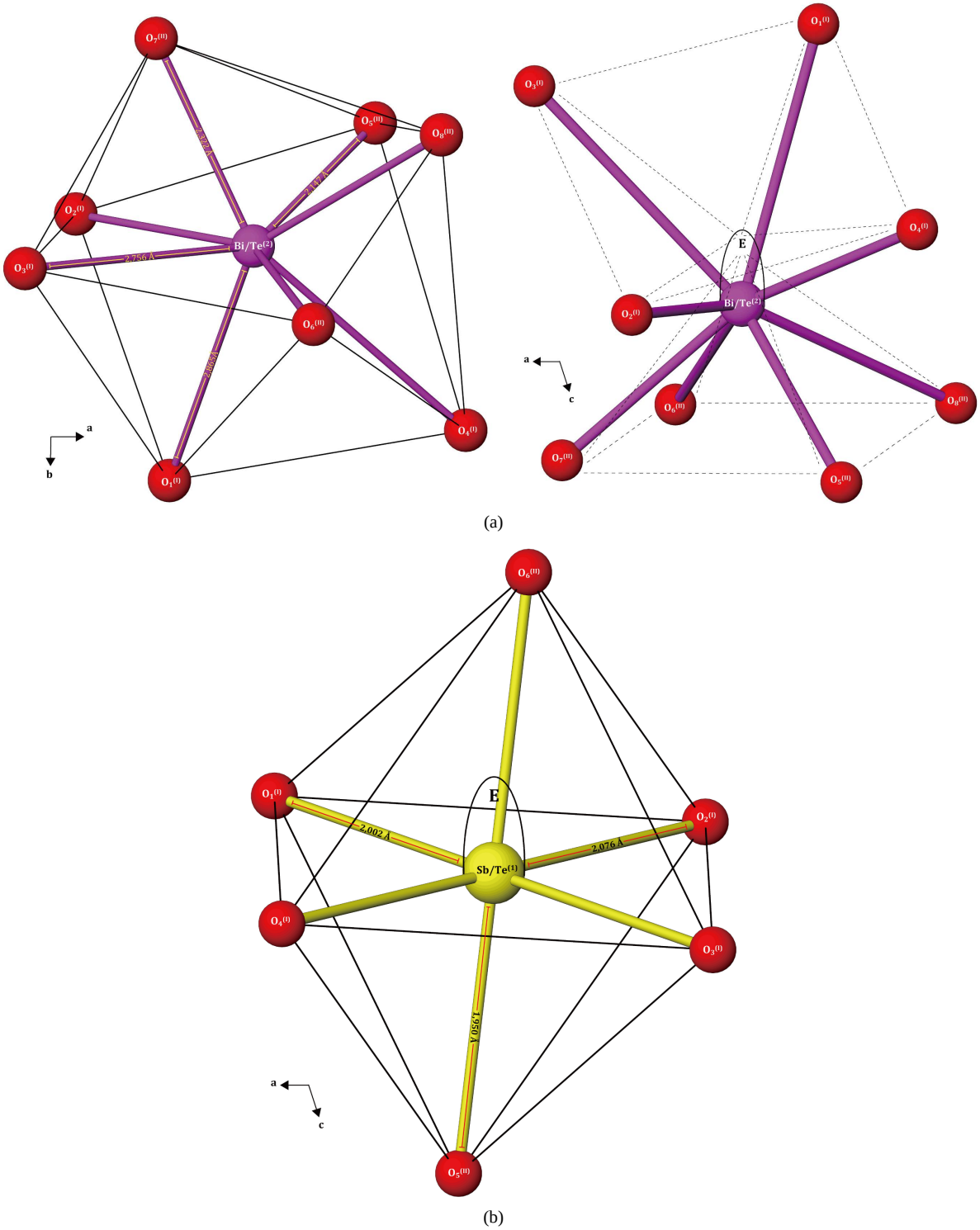

Figure 5. Spatial view of the $Bi/Te^{(2)}$ (a) and $Sb/Te^{(1)}$ (b) coordination.

and antimony ions Sb^{5+} by tellurium Te^{4+} contributes to increase the cationic disorder. It is interesting to note that the presence of tellurium oxide TeO_2 is minimal or it would create a distorted distribution of tellurium and antimony atoms in the same Wyckoff sites. The angle are 79.39˚ very close to those observed in β-Sb_2O_4 87.9 and 148.1˚ [7]. This result, show the $(SbTe^{(1)})O_6$ appears to be elongated. In the $(BiTe^{(2)})O_8$ polyhedron, however, the

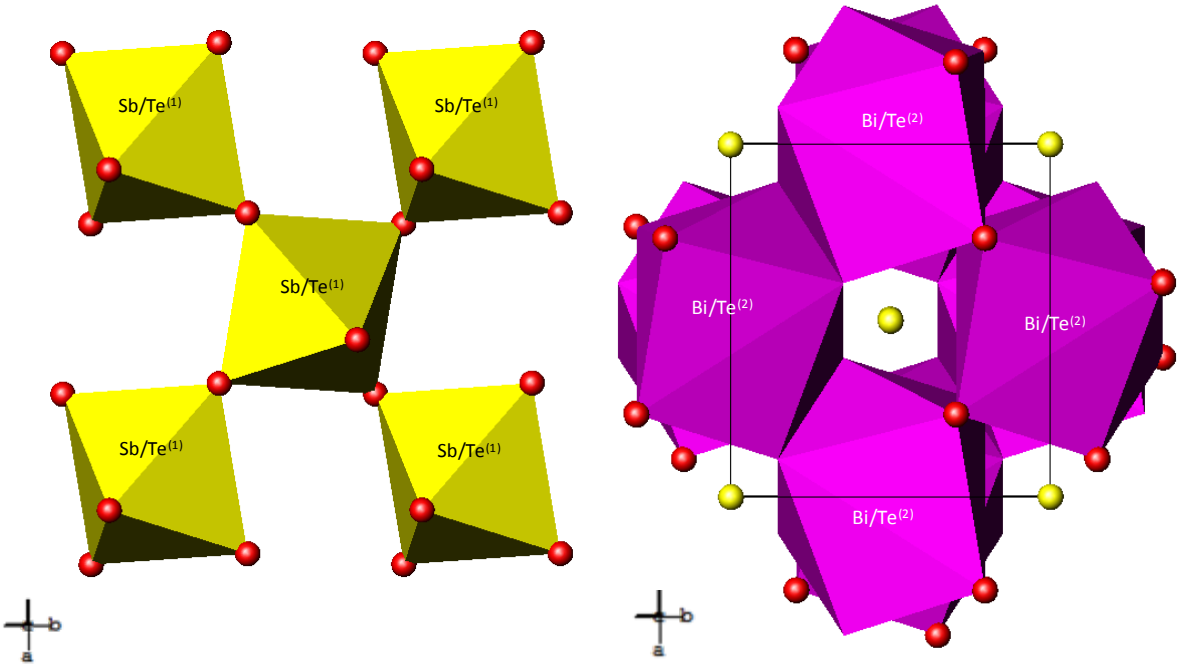

(a) (b)

Figure 6. A (001) projection showing the interconnection of $[(Sb/Te^{(1)})O_4]_n$ (a) and $(Bi/Te^{(2)})_2O_{14}$ (b) units in the $Bi_{0.90}Sb_{0.90}Te_{0.2}O_4$ crystal structure.

structural dissemetry results in a dipole moment. The bond-valence analyses [20] using the parameters by Brese and O'Keeffe [21] are in agreement with the expected values for different atoms. The results are summarized in **Table 4**. The antimony oxidation state is clearly +5 confirmed by a count of bond valence (**Table 4**). The electrostatic calculation of valence is not significant by taking account of The partial occupations of the 4c site is 0.9 and 0.1 for Bi and Te respectively and 0.9 and 0.1 for Sb and Te respectively for the 4d site. The theoreticals sum bond valence are (0.9 × 3) + (0.1 × 4) = 3.1 and (0.9 × 5) + (0.1 × 4) = 4.9 for 4c and 4d respectively. The experimental values are 3.38 and 5.04 for 4c and 4d respectively.

3.2. Vibrational Spectroscopy of $Bi_{1-x}Sb_{1-x}Te_{2x}O_4$ ($0 \le x \le 0.1$) Solid Solution

An attempt at building a database of Raman spectra of minerals was published [14]. The Raman spectra of $Bi_{1-x}Sb_{1-x}Te_{2x}O_4$ ($0 \le x \le 0.1$) are shown in **Figure 7**. For all samples, spectra obtained from different spots are identical. As reported by Cody, C. A *et al*. [22], β-Sb_2O_4 gives rise to Raman bands at 79 (medium), 94 (weak), 626 (medium), 142 (weak), 195 (medium, shoulder), 212 (very strong), 283 (weak), 405 (medium), 439 (weak), and a series of weak bands at 466, 635, and 754 cm^{-1}. Based on it relied on the existence of the totally symmetric vibration mode which is usually observed as the strongest band in the characteristic spectral region. This mode corresponds to the most covalent chemical bond of the anionic unit. The Raman spectra can be divided into three regions which correspond to $(Sb/Te^{(1)})$-O-$(Sb/Te^{(1)})$ vibrations (140 - 155 cm^{-1}), and connects $(Bi/Te^{(2)})$-O-$(Sb/Te^{(1)})$ at (395 - 450 cm^{-1}), vibration O-Bi^{3+}-O (740 - 790 cm^{-1}) and deformation O-Sb-O. In general the 770 antisymmetric stretch is found at a higher wavenumber than the symmetric stretch as observed in β-Sb_2O_4 [22] [23]. For example $CoSb_2O_6$ and $MgSb_2O_6$ two bands near 740 cm^{-1} in Raman correspond to deformation of Sb-Ob-Sb. The splitting is due to the slightly in equivalent bond lengths [24].

4. Conclusion

A new solid solution with formula $Bi_{1-x}Sb_{1-x}Te_{2x}O_4$ ($0 \le x \le 0.1$) is synthesized and its crystal structure has been determined using the Rietveld analysis of X-ray powder diffraction data. The new solid solution has a monoclinic symmetry and it presents a particularity to have a mixture of cations at the same site: $Bi/Te^{(2)}$ and

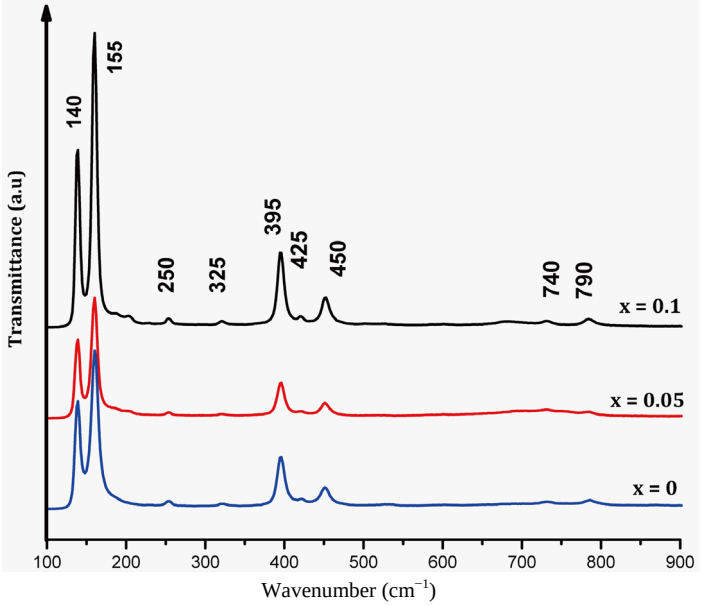

Figure 7. Raman spectra of crystalline phases of $Bi_{1-x}Sb_{1-x}Te_{2x}O_4$ solid solution with $0 \leq x \leq 0.1$ in the pseudo-binary $BiSbO_4$-TeO_2 system.

$Sb/Te^{(1)}$. The $(Sb/Te^{(1)})O_6$ octahedra are connected by sharing corners to form layers sheets. $Bi/Te^{(2)}$ atoms located in the interlayer are coordinated to eight atoms to form edge-sharing distorted $(Bi/Te^{(2)})O_8$ polyhedra. The crystal structure is constituted of layers $[Sb/Te^{(1)}]$ parallel to Oy which alternate in direction [101] with $(Bi(Te^{(2)})_2O_{14}$ units. The lone pair of Te and Bi are localized in opposite of shorts distance respectively. The coupled substitution of Bi^{3+} ions and antimony ions by Te^{4+} constitutes to increase the cationic distortion. The preliminary Raman study showed confirmed of solid solution and assigned three regions to O-Bi^{3+}-O, O-Sb^{5+}-O, connects $(Bi/Te^{(2)})O_8$-$(Sb/Te^{(1)})O_6$ and deformation modes vibration in the crystal.

References

[1] Keve, E.T. and Shapski, A.C. (1973) The Crystal Structure of Triclinic *β*-$BiNbO_4$. *Journal of Solid State Chemistry*, **8**, 159-165. http://dx.doi.org/10.1016/0022-4596(73)90009-1

[2] Subramanian, M.A. and Calabrese, J.C. (1993) Crystal Structure of the Low Temperature Form of Bismuth Niobium Oxide [*α*-$BiNbO_4$]. *Materials Research Bulletin*, **28**, 523-529. http://dx.doi.org/10.1016/0025-5408(93)90048-I

[3] Zhou, D., Wang, H., Yao, X., Wei, X.Y., Xiang, F. and Pang, L.X. (2007) Phase Transformation in $BiNbO_4$ Ceramics. *Applied Physics Letters*, **90**, Article ID: 172910. http://dx.doi.org/10.1063/1.2732833

[4] Zhou, D., Wang, H., Yao, X. and Pang, L.X. (2008) Dielectric Behavior and Cofiring with Silver of Monoclinic $BiSbO_4$ Ceramic. *Journal of the American Ceramic Society*, **91**, 1380-1383. http://dx.doi.org/10.1111/j.1551-2916.2008.02302.x

[5] Zhou, D., Wang, H., Yao, X. and Pang, L.X. (2008) Sintering Behavior, Phase Evolution, and Microwave Dielectric Properties of $Bi(Sb_{1-x}Ta_x)O_4$ Ceramics. *Journal of the American Ceramic Society*, **91**, 2228-2231. http://dx.doi.org/10.1111/j.1551-2916.2008.02462.x

[6] Lin, X.P., Huang, F.Q. and Zhang, K.L. (2006) A Novel Photocatalyst $BiSbO_4$ for Degradation of Methylene Blue. *Applied Catalysis A*: *General*, **307**, 257-262. http://dx.doi.org/10.1016/j.apcata.2006.03.057

[7] Kennedy, B. (1994) X-Ray Powder Diffraction Study of $BiSbO_4$. *Powder Diffraction*, **9**, 164-167. http://dx.doi.org/10.1017/S0885715600019151

[8] Tairi, A., Champarnaud-Mesjard, J.C., Mercurio, D., *et al*. (1985) Sur Quelques Phases Originales du Système Bi-Sb-O. *Revue De Chimie Minérale*, **22**, 699-710.

[9] Miyayama, M. and Yanagida, H. (1986) Oxygen Ion Conduction in *γ*-Bi_2O_3 Doped with Sb_2O_3. *Journal of Materials Science*, **21**, 1233-1236. http://dx.doi.org/10.1007/BF00553256

[10] Gribchenkova, N.A., Steblevskii, A.V., Kolosov, E.N., Alikhanian, A.S. and Nipan, G.D. (2007) High-Temperature Mass Spectrometric Vaporization Study of the Bi-Sb-O System. *Neorganicheskie Materialy*, **43**, 85-91.

[11] Chagraoui, A., Yakine, I., Tairi, A., Moussaoui, A., Talbi, M. and Naji, M. (2011) Glasses Formation, Characterization, and Crystal-Structure Determination in the Bi_2O_3-Sb_2O_3-TeO_2 System Prepared in an Air. *Journal of Materials Science*, **46**, 5439-5446. http://dx.doi.org/10.1007/s10853-011-5485-9

[12] Enjalbert, R., Sorokina, S., Castro, A. and Galy, J. (1995) Comparison of Bismuth Stereochemistry in (BiO_2)n and (Bi_2O_2)n Layers. Refinement of $BiSbO_4$. *Acta Chemica Scandinavica*, **49**, 813-819. http://dx.doi.org/10.3891/acta.chem.scand.49-0813

[13] Dowty, E. (2000) ATOMS for Windows: Version 5.1. Shape Software, Kingsport.

[14] Shannon, R.D. (1976) Revised Effective Ionic Radii and Systematic Studies of Interatomic Distances in Halides and Chalcogenides. *Acta Crystallographica*, **A32**, 751-767.

[15] Rogers, D. and Skapski, A.C. (1964) *Proceedings of the Chemical Society*, 400-401.

[16] Alonso, J.A., Castro, A., Enjalbert, R., Galy, J. and Rasines, I. (1992) The Quadruple Chains of SbO_6 Octahedra in $Sb_2Te_2O_9$: An Example of Low Extent of Aggregation of Penta-Valent Antimony Polyhedra. *Journal of the Chemical Society*, *Dalton Transactions*, 2551.

[17] Champarnaud-Mesjard, J.C., Frit, B., Chagraoui, A. and Tairi, A. (1996) Crystal Structure of a New Cation-Ordered Fluorite-Related Phase: $Bi_2Te_2WO_{10}$. *Zeitschrift für Anorganische und Allgemeine Chemie*, **622**, 1907-1912. http://dx.doi.org/10.1002/zaac.19966221116

[18] Champarnaud-Mesjard, J.C., Frit, B., Chagraoui, A. and Tairi, A. (1996) New Anion-Excess, Fluorite-Related, Ordered Structure: $Bi_2Te_2W_3O_{16}$. *Journal of Solid State Chemistry*, **127**, 248-255. http://dx.doi.org/10.1006/jssc.1996.0381

[19] Chagraoui, A., Tairi, A. and Champarnaud-Mesjard, J.C. (2006) Crystal Structure of a New Stoichiometric Compound: $Bi_2Te_5WO_{16}$ Deriving from Fluorite Type. *Journal of Physics and Chemistry of Solids*, **67**, 2241-2252. http://dx.doi.org/10.1016/j.jpcs.2006.04.016

[20] Brown, J.D. (2002) The Chemical Bond in Inorganic Chemistry. Oxford University Press, Oxford.

[21] Brese, N.E. and O'Keeffe, M. (1991) Bond-Valence Parameters for Solids. *Acta Crystallographica Section B*: *Structural Science*, **47**, 192-197. http://dx.doi.org/10.1107/S0108768190011041

[22] Cody, C.A., DiCarlo, L. and Darlington, R.K. (1979) Vibrational and Thermal Study of Antimony Oxides. *Inorganic Chemistry*, **18**, 1572-1576. http://dx.doi.org/10.1021/ic50196a036

[23] Mestl, G., Ruiz, P., Delmon, B. and Knözinger, H. (1994) Sb_2O_3/Sb_2O_4 in Reducing/Oxidizing Environments: An *in Situ* Raman Spectroscopy Study. *The Journal of Physical Chemistry*, **98**, 11276-11282. http://dx.doi.org/10.1021/j100095a008

[24] Albrecht-Schmitt, T.E., Sykora, R.E., King, J.E. and Illies, A.J. (2004) Hydrothermal Synthesis, Structure, and Catalytic Properties of $UO_2Sb_2O_4$. *Journal of Solid State Chemistry*, **177**, 1717-1722. http://dx.doi.org/10.1016/j.jssc.2003.12.033